agronomy

MDPI

Article

Antimicrobial Potential of Essential Oils from Aromatic Plant *Ocimum* sp.; A Comparative Biochemical Profiling and In-Silico Analysis

Prafull Salvi [1,*,†], Gulshan Kumar [1,†], Nishu Gandass [1], Kajal [1], Ashish Verma [2], Sivasubramanian Rajarammohan [1], Nilesh Rai [2] and Vibhav Gautam [2]

[1] Agri-Biotechnology, National Agri-Food Biotechnology Institute, Mohali 140306, India; gulshan.ihbt@gmail.com (G.K.); nishukarate3198@gmail.com (N.G.); mittalkajal003@gmail.com (K.); siva.r24@nabi.res.in (S.R.)

[2] Centre of Experimental Medicine and Surgery, Institute of Medical Sciences, Banaras Hindu University, Varanasi 221005, India; ashishambbhu@gmail.com (A.V.); nilesh.rai17@bhu.ac.in (N.R.); vibhav.gautam4@bhu.ac.in (V.G.)

* Correspondence: salvi.prafull@gmail.com

† These authors contributed equally to this work.

Abstract: Medicinal and aromatic plants (MAPs) are a rich source of bioactive compounds that are immensely important due to their potential use in pharmacological and agricultural applications. Here, we have evaluated the antimicrobial activity of essential oils (EOs) from three different species of *Ocimum*: *O. gratissimum* (EO1), *O. tenuiflorum* (EO2), and *O. sanctum* (EO3). The EOs were screened for antibacterial activity against pathogenic strains of *Escherichia coli*, *Enterobacter cloacae* and methicillin-resistant *Staphylococcus aureus* (MRSA). The essential oils EO1 and EO3 showed significant growth inhibition of the tested bacteria. Likewise, all EOs exhibited antifungal potential against the broad-spectrum plant fungal pathogen *Sclerotinia sclerotiorum* that causes white-mould disease in plants. Moreover, the antimicrobial potential of the EOs correlates well with their antioxidant activity determined by DPPH free radical scavenging activity. The biochemical analysis of the EOs employing high-performance thin-layer chromatography, gas chromatography-mass spectrometry, and Fourier transform infrared spectroscopy, revealed the presence of distinct phytoconstituents that might be responsible for their differential bioactivity. Furthermore, an in-silico evaluation of the candidate phytoconstituents using molecular docking analysis suggests their potential for antimicrobial applications. Altogether, our results clearly show that EO1 and EO3 possess promising antimicrobial properties, and therefore could be utilized as a potential antimicrobial agent.

Keywords: *Ocimum* sp.; essential oil; antimicrobial; HPTLC; GC-MS; FTIR; molecular docking; crop protection

Citation: Salvi, P.; Kumar, G.; Gandass, N.; Kajal; Verma, A.; Rajarammohan, S.; Rai, N.; Gautam, V. Antimicrobial Potential of Essential Oils from Aromatic Plant *Ocimum* sp.; A Comparative Biochemical Profiling and In-Silico Analysis. *Agronomy* **2022**, *12*, 627. https://doi.org/10.3390/agronomy12030627

Academic Editors: Alessandra Carrubba and Mauro Sarno

Received: 24 January 2022
Accepted: 24 February 2022
Published: 4 March 2022

1. Introduction

Medicinal and aromatic plants (MAPs) contain a plethora of bioactive pharmacological compounds that endow enormous beneficial effects and support ecological as well as economical benefits [1,2]. As their name implies, aromatic plants possess aromatic compounds, more precisely, these comprise essential oils (EO). Essential oils are a secondary metabolite produced by plants in different tissues including the root, shoot, leaf, flower, bark, fruit, peel, etc. that support the plant growth, propagation and defence system [3,4]. The EOs are highly volatile and hydrophobic in nature, and are known for flavour, aromas and antimicrobial activity that showcase them as an appeasing asset for commercial purposes. The EOs are composed of a complex mixture of several low molecular weight (10 to 100 kDa) terpenoids and phenylpropenes in varied concentration. Although the major chemical constituents of EOs largely impact their properties, the constituents present in

traces may also significantly influence their bioactivity including aroma and flavour [5–7]. The growing corpus of evidence have shown that the constituents of EOs enhance the diversity of the plant's secondary metabolites to endure the pathogenesis [8–10]. Besides, these constituents are also known to have a beneficial impact on growth, and thus are referred as bio-stimulants. The genus *Ocimum* sp. (tulsi) of the *Lamiaceae* family, encompasses about 150 species that are widely known for their diverse phytoconstituents employed in aromatherapy, phytomedicine, food and cosmetic industry [11,12]. Eugenol, rosmarinic acid, carvacrol and oleanolic acid are some of the bioactive secondary metabolites of *Ocimum* sp. [13,14]. The medicinal use of *Ocimum* sp. has been known since the Vedic period (3500–1600 B.C.), however the beneficial role of its phytoconstituents in crop protection remains poorly understood [15,16].

Plants exposure to (a)biotic stress, including extreme temperatures, drought, flooding, bacterial and fungal infection, etc., disturbs cellular functionality that limits their growth and development and eventually reduces the crop yield and quality. These stressors disturb the cellular and metabolic processes by altering the phytohormone signalling, transcriptional regulation, and signalling cascade, which eventually results in compromised growth and productivity of plants [17–21]. The impact of biotic stress has resulted in a huge loss to the global economy and intensifies the issues of hunger and food insecurity. Therefore, to ensure sustainability in a plant-based economy, it is of utmost importance to adopt effective strategies that can restrict the losses associated with biotic stress. Several agrochemicals are in use to circumvent the issue of losses associated with biotic stress, however, the injudicious use of such hazardous agrochemicals has resulted in their accrual in the food chain that has raised environmental and human health concerns [22,23]. Several research studies have documented the use of essential oils as pesticides. Because pesticides obtained from plants sources would have high volatile potential, less persistency, and low toxicity to vertebrates, they are safer in terms of health concerns and environmental impact [24].

In the present study, we investigated the antibacterial and antifungal potential of EOs extracted from three different species of *Ocimum*. Particularly, we examined the antimicrobial activity of these EOs against a broad-spectrum fungal plant pathogen *Sclerotinia sclerotiorum*, that severely curtails the yield potential of diverse plant species including dry bean, soybean, canola, sunflower, peanut, etc. [25–27]. To identify the constituent phytochemicals of EOs, their chemical characterization was performed using analytical methods including HPTLC, GC-MS, and FT-IR. The phytoconstituents were further evaluated for their potential antimicrobial roles using a molecular docking approach. The in-silico docking analysis of selected phytoconstituents of EOs was assessed for their molecular interaction with the vital cellular enzymes of bacteria and studied their antibacterial role.

2. Materials and Methods

2.1. Plant Material and Essential Oil Used

The EOs were obtained from the Centre for Aromatic Plants, Dehradun, India, a premier institute involved in conservation, cultivation, processing, and quality assessment of aromatic plants. The specific gravity of the EOs of *O. gratissimum*, *O. tenuiflorum*, and *O. sanctum*, was determined to be 0.9645, 0.891, and 0.92, respectively.

2.2. Chemical Characterization of EOs

High-performance thin-layer chromatography (HPTLC) fingerprinting, gas chromatography-mass spectrometry (GC-MS) and Fourier transform infrared (FTIR) spectrum analysis were performed to elucidate the chemical composition of the EOs. The HPTLC was performed on 10 × 10 cm size of TLC (Thin layer chromatography) plates (Merck, Germany) using CAMAG HPTLC equipment (ANCHROM, Muttenz, Switzerland) composed of a Linomat-4 autosampler, CAMAG TLC scanner-4 and visualizer. For chromatographic separation of the EOs constituents, toluene: chloroform: ethyl alcohol (4:4:1 $v/v/v$) was used as a mobile phase. The scanning of the TLC plate was performed on a TLC scanner-4 (Instrument source) at 254 nm and 366 nm. The area percentage and retention factor for the

separated components was calculated using winCATS Planar Chromatography Manager (version 1.4.10.0001). For visualization of separated components on the TLC plate, post-chromatographic derivatization was performed using anisaldehyde sulphuric acid (AS) reagent (170 mL pre-cooled methanol, 20 mL acetic acid, 10 mL sulphuric acid and 1 mL anisaldehyde). The derivatized TLC plate was then scanned at 570 nm and the image was captured using TLC scanner-4 at 570 nm.

The GC–MS analyses of all EOs were performed on Agilent 7890 GC system coupled to a 7000 EI-MS system (Agilent Technologies, Santa Clara, CA, USA). A DB-5 silica capillary column (60 m × 250 µm, 1 µm film thickness) was used for the chromatographic separation using the following temperature profile: 80 °C for 2 min, 80 to 220 °C at 4 °C min^{-1}, 220 °C for 2 min, 220 to 300 °C at 10 °C min^{-1}, 300 °C for 2 min. The helium was used as carrier gas at a flow rate of 1.5 mL min^{-1}. The mass spectra were recorded in the total ion chromatogram mode with m/z range of 30–550. The split ratio for all the analysed samples was set at 1:50 for 1 µL injection. The Fourier transform infrared (FTIR) spectrum analysis of the EOs was performed on a PerkinElmer Spectrum Version 10.5.2 in the range of 4000–450 cm^{-1} [28,29].

2.3. Antimicrobial Activity

The antimicrobial activity of the EOs was determined by employing a disc diffusion method against two gram-negative bacteria viz. *Escherichia coli* (ATCC 11775) and *Enterobacter cloacae* (ATCC 13047) and, one gram-positive bacteria viz. methicillin resistant *Staphylococcus aureus* (ATCC 33591). The plates were initially left for 30 min at 10 °C to allow the diffusion of the EOs before they were incubated for 24–48 h at 37 °C for bacterial growth. Chloramphenicol discs (10 mcg) were used as a positive control and were also used to calculate the relative antibacterial activity. The clear zones of growth inhibition around the discs indicates the antibacterial activity against the test organism.

Similarly, a disc diffusion assay was performed to determine the antifungal activity of the EOs against the plant fungal pathogen *S. sclerotiorum*. The 2 mm of fungal strain was punched and placed in the middle of each Petri dish containing the EO impregnated disc and incubated at 25 °C for 7 days. Discs impregnated with 0.5% DMSO were used as a solvent control. The fungal growth zone was observed daily, and their diameters measured. The comparison of the diameters of fungal growth obtained with those of the control was employed to calculate the percentage of inhibition at day 7, according to the following formula:

$$\% \text{ inhibition} = \frac{(Growth\ diameter\ in\ control - Growth\ diameter\ in\ treatment)}{Growth\ diameter\ in\ control} \times 100$$

All the experiments for antimicrobial activity were performed in triplicate. The student's *t*-test was performed to evaluate the significance level of the observed value to that observed for the EO1.

2.4. Antioxidant Activity Assay

The in vitro antioxidant activity of the EOs was measured by its ability scavenge DPPH free radicals following the method of [30]. The antioxidant activity of EOs was determined using the absorbance (A) measured at 517 nm and calculated as DPPH free radical scavenging activity (%) = [A(blank) − A(sample)]/A(blank) × 100%. The analysis was performed in triplicate, each with three technical replicates.

2.5. Molecular Docking Analysis

To determine the interaction of the EOs phytoconstituents with the microbial target proteins, we performed in-silico interaction analysis using AutoDock Vina [31]. The three-dimensional structure of the target proteins was retrieved from Protein Data Bank (PDB) database. The Swiss-Pdb Viewer was used for energy minimization of target proteins [32]. The target proteins were prepared for docking by removing co-crystallized ligands, water

molecules, and by adding hydrogen atoms. The three-dimensional structure of ligand compounds was retrieved from PubChem tool (https://pubchem.ncbi.nlm.nih.gov/, accessed on 10 November 2021). The energy minimization of ligand compounds was done using UCSF Chimera tool (http://www.cgl.ucsf.edu/chimera, accessed on 17 November 2021), and refinement was performed using AutoDock 4.2 tool [33]. The interactions with strong binding affinity were selected for visualization using PyMol and discovery studio visualizer.

3. Results and Discussion

3.1. Biochemical Characterization of EOs

The EOs from *O. gratissimum*, *O. tenuiflorum*, and *O. sanctum* were named as EO1, EO2 and EO3, respectively. To determine the biochemical profile of EOs, we employed three analytical methods viz. HPTLC, GC-MS, and FTIR, to determine the EO's composition, constituent annotation, and functional groups, respectively. For HPTLC fingerprinting, we screened different combinations of polar and nonpolar solvents; toluene: chloroform: ethyl alcohol (4:4:1 $v/v/v$) resulted in excellent chromatographic resolution of the EO constituents. The TLC plate was scanned at 254 nm and 366 nm, and derivatized with AS reagent to reveal the distinct chemical composition of all the EOs. For instance, scanning at 254 nm revealed the presence of 11 peaks representing the different biochemical constituents in EO1, while EO2 had only five peaks, and EO3 had eight distinct peaks (Figure 1). Moreover, the peaks number and their area revealed the high heterogeneity of EO1 in terms of its constituent biochemicals, and this heterogeneity was further followed by EO3 and EO2 (Figure 1). Briefly, six peaks in EO1 represented nearly 91% of total peaks area, while only three peaks (mention Rf) in EO2 covered nearly 89% of total peak area, whereas four peaks in EO3 represented 93% of total peaks area. The scanning of the same TLC plate at 366 nm corroborated the high heterogeneity of EO1 (seven peaks), and less in EO2 and EO3 (five peaks each). Four peaks in EO1 represented 90.77% of the total peaks area, while three peaks separately in EO2 and EO3 each covered almost 89.9% and 96%, respectively. Interestingly, the comparison of retardation factor (Rf) values indicated sharing of some biochemical entities in EO1 and EO3, and this suggests a similarity between the EO1 and EO3 (Figure 1). Usually, the AS-based derivatization indicates the chemical nature of bioactive components such as terpenoid, steroids, sterols and saponins present in a plant tissue extract. We observed different colours of bands in EO1 upon AS-based derivatization, where a pinkish violet colour band indicated the presence of glycosides, a bluish violet colour indicated terpenoids, and a green colour indicated the presence of saponins observed through derivatization of the TLC plate. A yellow colour band in EO2 and a blue colour band in EO2 and EO3, respectively, suggested the presence of saponins.

Although the HPTLC revealed the biochemical distinctiveness of the three EOs, for the detailed biochemical profiling of the constituent compounds, we performed GC-MS analysis. The GC-MS analysis resulted in the identification of more than 100 diverse compounds in all the three EOs examined (Table 1 and Figure 2). In agreement with the HPTLC data, the GC-MS analysis also revealed the heterogeneity of EOs that followed the order of EO1 > EO3 > EO2; 14 constituents in EO1, 12 constituents in EO3, and 10 constituents in EO2 have relative abundances of $\geq$2.5% of the total identified compounds in respective samples. The total number of identified constituents were comparable in EO1 and EO2, 47 and 48 respectively, while EO3 had only 41 compounds identified in total. The results also revealed that the compounds present in higher percentage belong mostly to the classes of monoterpenes, sesquiterpenes, octahydronaphthalenes, and benzopyran derivatives. Indeed, the compounds having >4% of relative abundance were different in each EO; 6-Isopropenyl-4,8a-dimethyl-1,2,3,5,6,7,8,8a-octahydro-naphthalen-2-ol (16.22%), Phenol, 2-methoxy-3-(2-propenyl)- (14.71%), γ-Muurolene (6.57%), 9-Methoxycalamenene (6.51%), β-Pinene (4.86%), Aromadendrene oxide-(1) (4.21%), and Ylangene (4.09%) were the most abundant constituents of EO1; while α-Guaiene (20.78%), 2H-1-Benzopyran, 3,4,4a,5,6,8a-hexahydro-2,5,5,8a-tetramethyl-(2α,4aα,8aα)- (12.15%), α-Selinene (10.84%), β-Guaiene (5.03%), Germacrene D (4.82%), β-Cubebene (4.49%), 1,2,3,4,6,7,8,8a-Octahydronaphthalene-6,7-diol,

5,8a-dimethyl-3-isopropenyl-, cyclic carbonate, trans- (4.35%), and Selina-3,7(11)-diene (4.11%) were the most abundant constituents of EO2, whereas α-Citral (14.75%), Cyclohexane,1-ethenyl-1-methyl-2,4-bis(1-methylethenyl)-, [1S-(1α,2β,4β)]- (11.81%), Caryophyllene (8.91%), Phenol,2-methoxy-3-(2-propenyl)- (8.52%), α-Amorphene (7.78%), γ-Muurolene (7.43%), and 2*H*-1-Benzopyran,3,4,4a,5,6,8a-hexahydro-2,5,5,8a-tetramethyl-(2α,4aα,8aα)- (4.52%). Among these constituents, only the Phenol, 2-methoxy-3-(2-propenyl)- and 1-Benzopyran,3,4,4a,5,6,8a-hexahydro-2,5,5,8a-tetramethyl-(2α,4aα,8aα)- were shared in either of the EO combinations. Our results are in agreement with the chemical composition analysis observed in previous studies [29,34]. All the identified chemical constituents of EOs are listed in Table 1.

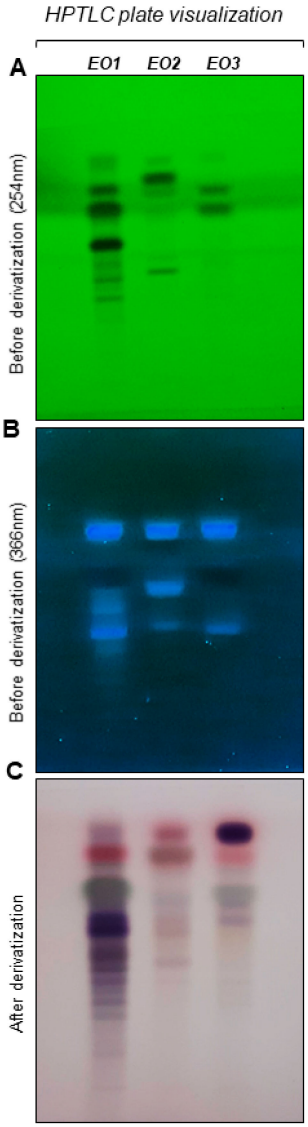

Peak integration Rf value and peak area

Peak	EO1		EO2		EO3	
	Rf	Area (%)	Rf	Area (%)	Rf	Area (%)
1	0.14	0.39	0.4	10.08	0.33	0.85
2	0.21	0.5	0.53	5.82	0.37	1.57
3	0.27	1.71	0.66	23.34	0.42	1.3
4	0.33	1.5	0.79	55.24	0.46	9.53
5	0.37	4.44	0.94	5.52	0.6	3.27
6	0.42	11.44	-	-	0.67	46.72
7	0.51	7.6	-	-	0.8	30.5
8	0.56	23.45	-	-	0.93	6.27
9	0.68	28.68	-	-	-	-
10	0.82	13.07	-	-	-	-
11	0.9	7.22	-	-	-	-

Peak	EO1		EO2		EO3	
	Rf	Area (%)	Rf	Area (%)	Rf	Area (%)
1	0.3	2.5	0.46	2.11	0.18	0.59
2	0.43	3.66	0.51	8.33	0.46	11.95
3	0.47	19.51	0.61	27.26	0.63	7.66
4	0.65	8	0.77	7.97	0.77	3.27
5	0.78	3.06	0.91	54.33	0.87	76.52
6	0.88	5.51	-	-	-	-
7	0.93	57.75	-	-	-	-

Peak	EO1		EO2		EO3	
	Rf	Area (%)	Rf	Area (%)	Rf	Area (%)
1	0.21	7.29	0.2	2.77	0.16	0.79
2	0.32	2.6	0.32	5.89	0.31	0.96
3	0.35	2.69	0.45	3.45	0.35	2.08
4	0.4	1.39	0.5	4.27	0.52	34.04
5	0.43	2.6	0.55	32.82	0.75	62.13
6	0.47	5.86	0.74	33.56	-	-
7	0.53	6.54	0.91	9.25	-	-
8	0.64	8.87	0.96	7.99	-	-
9	0.79	55.88	-	-	-	-
10	0.94	6.29	-	-	-	-

Figure 1. Developed HPTLC plate photograph of essential oil from *O. gratissimum* (EO1), *O. tenuiflorum* (EO2), and *O. sanctum* (EO3). (**A**) 254 nm before derivatization (**B**) 366 nm before derivatization (**C**) Visible mode after derivatization.

Table 1. GC-MS analysis of essential oil from *O. gratissimum* (EO1), *O. tenuiflorum* (EO2), and *O. sanctum* (EO3).

Compound Name	% Area of the Peak		
	EO1	**EO2**	**EO3**
6-Isopropenyl-4,8a-dimethyl-1,2,3,5,6,7,8,8a-octahydro-naphthalen-2-ol	16.22	-	-
Phenol, 2-methoxy-3-(2-propenyl)-	14.71	0.34	8.52
γ-Muurolene	6.57	0.77	7.43
9-Methoxycalamenene	6.51	-	-
β-Pinene	4.86	0.99	1.09
Aromadendrene oxide-(1)	4.21	-	-
Ylangene	4.09	-	-
3-Cyclohexen-1-ol, 4-methyl-1-(1-methylethyl)-, (R)-	3.01	-	0.61
α-Muurolene	2.90	1.48	-
2,6-Octadienal, 3,7-dimethyl-, (Z)-	2.78	-	-
Eremophilene	2.74	-	-
Caryophylene oxide	2.67	0.43	0.66
β-trans-Ocimene	2.50	-	1.48
β-Bourbonene	2.48	-	-
Cyclohexane, 2-ethenyl-1,1-dimethyl-3-methylene-	2.27	-	-
β-Ocimene	1.60	-	-
Bicyclo[3.1.0]hexan-2-ol, 2-methyl-5-(1-methylethyl)-, (1α,2α,5α)-	1.60	0.24	-
δ-Cadinene	1.45	-	-
Benzeneethanamine, α-methyl-	1.34	-	-
α-Caryophyllene	1.25	-	0.50
αthujene	1.15	-	-
2-Methylbicyclo [4.3.0] non-1(6)-ene	1.09	-	-
1H-Benzocyclohepten-7-ol, 2,3,4,4a,5,6,7,8-octahydro-1,1,4a,7-tetramethyl-, cis-	1.09	-	-
Selina-3,7(11)-diene	1.06	4.11	-
β-Caryophyllene epoxide	0.99	-	-
2,6-Dimethyl-1,3,5,7-octatetraene, E,E-	0.91	0.72	-
γ-Terpinen	0.72	-	0.82
3-Cyclohexene-1-methanol, α,α4-trimethyl-	0.67	-	-
α-Phellandrene	0.65	-	0.36
Naphthalene, 1,2,3,4,6,8a-hexahydro-1-isopropyl-4,7-dimethyl-	0.61	0.24	-
Bicyclo[3.1.0]hex-2-ene, 4,4,6,6-tetramethyl-	0.58	-	-
Alloaromadendrene oxide-(1)	0.48	-	-
3,7-Octadiene-2,6-diol, 2,6-dimethyl-	0.33	-	-
cis-p-Mentha-2,8-dien-1-ol	0.28	-	-
Methyl 4,7,10,13-hexadecatetraenoate	0.26	-	-

Table 1. *Cont.*

Compound Name	% Area of the Peak		
	EO1	**EO2**	**EO3**
β-Cubebene	0.25	4.49	-
Linalool	0.25	-	-
Tricyclo[5.2.2.0(1,6)]undecan-3-ol, 2-methylene-6,8,8-trimethyl-	0.24	-	-
Tau-Cadinol	0.23	-	-
Aromadendrene oxide-(2)	0.23	0.37	-
Aristolene epoxide	0.22	-	-
Eugenol	0.22	-	-
β-Phellandrene	0.18	1.39	0.22
1S-α-Pinene	0.18	-	-
α-Cadinol	0.18	0.38	-
β-Caryophyllene	0.17	1.76	-
α-Guaiene	-	20.78	-
2H-1-Benzopyran, 3,4,4a,5,6,8a-hexahydro-2,5,5,8a-tetramethyl-(2α,4aα,8aα)-	-	12.15	4.52
α-Selinene	-	10.84	-
β-Guaiene	-	5.03	-
Germacrene D	-	4.82	0.18
1,2,3,4,6,7,8,8a-Octahydronaphthalene-6,7-diol, 5,8a-dimethyl-3-isopropenyl-, cyclic carbonate, trans-	-	4.35	-
α-Citral	-	3.37	14.75
Globulol	-	2.47	-
β-Citral	-	2.28	2.53
β-Selinene	-	1.65	0.24
Camphene	-	1.34	1.53
1R,4S,7S,11R-2,2,4,8-Tetramethyltricyclo[5.3.1.0(4,11)]undec-8-ene	-	1.13	-
o-Menth-8-ene, 4-isopropylidene-1-vinyl-	-	1.00	0.70
(−)-β-Elemene	-	0.95	-
Borneol	-	0.92	0.21
Cyclohexene, 1-methyl-4-(1-methylethylidene)-	-	0.80	-
Cadina-1(10),4-diene	-	0.71	-
Isocaryophillene	-	0.70	-
α-Humulene	-	0.62	2.74
γ-Cadinene	-	0.61	-
Androstan-17-one, 3-ethyl-3-hydroxy-, (5α)-	-	0.60	-
Isoaromadendrene epoxide	-	0.60	-
1R-α-Pinene	-	0.52	3.11
n-Amyl isovalerate	-	0.50	-
(+)-Cyclosativene	-	0.46	-
Terpinolene	-	0.45	0.88

Table 1. *Cont.*

Compound Name	% Area of the Peak		
	EO1	EO2	EO3
(+)-Sativene	-	0.45	-
Bicyclo[2.2.1]heptan-2-one, 1,7,7-trimethyl-, (1S)-	-	0.44	-
Benzene, 4-allyl-1,2-dimethoxy-	-	0.40	-
D-Limonene	-	0.31	1.15
Geranyl vinyl ether	-	0.27	-
7(11)-Selinen-4α-ol	-	0.27	0.74
1,5-Dimethyl-1-vinyl-4-hexenyl butyrate	-	0.27	-
Cubenol	-	0.26	-
Cyclohexane, 1-ethenyl-1-methyl-2,4-bis(1-methylethenyl)-, [1S-(1α,2β,4β)]-	-	-	11.81
Caryophyllene	-	-	8.91
α-Amorphene	-	-	7.78
2-Isopropenyl-4a,8-dimethyl-1,2,3,4,4a,5,6,7-octahydronaphthalene	-	-	3.44
Juniper camphor	-	-	2.95
β-Elemene	-	-	2.26
Isoborneol	-	-	1.54
γ-Gurjunene	-	-	1.14
α-Longipinene	-	-	1.04
Guaia-1(10),11-diene	-	-	0.94
Epiglobulol	-	-	0.90
α-Terpinen	-	-	0.68
α-Panasinsen	-	-	0.51
Furan, 2,5-diethyltetrahydro-	-	-	0.30
Selina-6-en-4-ol	-	-	0.29
4(10)-Thujene	-	-	0.20
Octanal	-	-	0.17
Eucalyptol	-	-	0.16

Further, we performed a FT-IR analysis to investigate the presence of functional groups. The essential oils are a complex mixture of various volatile compounds, and their IR spectra generally overlaps for various components. The spectral region from 600 cm^{-1} to 1700 cm^{-1} represents the characteristic IR fingerprint of *Ocimum* oil (Figure 3) [35]. The IR spectra further corroborate the compositional similarity of EO1 and EO3 as determined through HPTLC; most of the IR absorption wavenumbers were similar in EO1 and EO3. The EO3 have additional peaks to that of EO1 at wave numbers 886 cm^{-1} and 1613 cm^{-1} and represents the C=C bending and stretching of alkene α-β-unsaturated ketones, respectively. In contrast, the EO2 has several distinct peaks to that of EO1 and EO3, such as at wave numbers 765 cm^{-1}, 804 cm^{-1}, 953 cm^{-1}, 1029 cm^{-1}, 1139 cm^{-1}, 1153 cm^{-1}, 1189 cm^{-1}, 1234 cm^{-1}, 1259 cm^{-1}, 1337 cm^{-1}, 1418 cm^{-1} and 1591 cm^{-1} that represent the stretching or bending vibrations of C–H, O–H, C–O bonds of alkenes, alcohols, ether, and might correspond to some volatile terpenoids [36,37]. The peak at wave number 1266 cm^{-1} is attributed to C–O stretching vibration of aromatic ester. The sharp peak at wave number 1367 cm^{-1} in

EO1 and EO3 represent the phenolic group of Phenol, 2-methoxy-3-(2-propenyl)- present at higher percentage in both as compared to that of EO2. The peak at wave number 1451 cm^{-1} is a very characteristic for C–H bending vibration of methyl group. In addition, the sharp peak at wave number 1512 cm^{-1} in all the EOs represent the stretching of C=C of aromatic compounds. Likewise, the peaks at 1638 cm^{-1} correspond to the C=C stretching vibration of conjugated alkenes. Altogether, all the EOs compositions exhibit much complexity and diversity, as shown in Figure 3.

3.2. Antimicrobial Activity and Antioxidant Activity of EOs

To evaluate the bioactivity of the EOs, we investigated their antimicrobial activity against pathogenic bacterial strains viz. *E. coli* (ATCC 11775), *E. cloacae* (ATCC 13047), and methicillin-resistant *S. aureus* (ATCC 33591). Interestingly, all the EOs exhibited antibacterial activity against the tested bacterial strains, however they showed varied growth inhibition. The EO1 and EO3 significantly inhibited the growth of gram-negative *E. coli* and *E. cloacae*. The EO1 exhibited highest growth inhibition potential against *E. coli* in a concentration ranging from 50% to 12.5% (*v*/*v*) (Figure 4A). The antibacterial activity of EO1 against *E. coli* was followed by EO3, however to a lesser extent, while the EO2 had the least potential to inhibit the *E. coli* growth (Figure 4A). Unexpectedly, the EO1 and EO3 were found to have comparable antibacterial activity against the *E. cloacae* (Figure 4B). Here, the EO2 at higher concentration also resulted in growth inhibition of *E. cloacae*, however less than that of other EOs. From these observations, it is reasonably likely that EO1 and EO3 would have anti-MRSA activity against methicillin resistant *S. aureus* (MRSA). Intriguingly, as expected, the EO1 and EO3 both exhibited anti-MRSA activity (Figure 4C). Although, a significant anti-MRSA activity of EO1 and EO3 was observed across the dilution range, the higher dilution of EO3 had slightly more anti-MRSA activity than that of EO1. The EO2 anti-MRSA activity was tenuous, much alike to its antibacterial activity against *E. coli* and *E. cloacae* (Figure 4A, 4B). Altogether, all three essential oils exhibited antibacterial activity against the bacterial strains used in the present study. From the serial dilution of EOs, EO1 showed potent antibacterial activity in the range of 6.25% to 25% (*v*/*v*), whereas EO2 and EO3 showed in the range 25% (*v*/*v*) and 12.5 to 25% (*v*/*v*), respectively. The minimum inhibitory concentration (MIC) of three EOs against these bacterial test strains was evaluated by microdilution method in the concentration range from 50% to 0.097% (*v*/*v*) (Table 2) [38].

Unlike for their antibacterial activity, to our surprise, all the EOs were found to exhibit strong antifungal activity against the fungal plant pathogen *S. sclerotiorum* (Figure 4D). The direct use of concentrated EO was able to completely inhibit the growth of *S. sclerotiorum*. Further, the 1:10 and 1:100 dilutions of the EOs suggests that the antifungal potential of the EOs follows the same order as that of the antibacterial activity; EO1 > EO3 > EO2. Previously, it was reported that the EO bioactive constituents of *O. sanctum*, such as methyl chavicol and linalool, disturb the membrane integrity in fungus *Candida* by affecting ergosterol biosynthesis, and thus displayed antifungal activity [39]. Recently, Žabka et al. [40] evaluated the antifungal and insecticidal roles of *O. sanctum* EO on restricting the growth of several pathogenic fungal isolates including *Aspergillus flavus*, *Penicillium expansum*, and *Fusarium verticillioides*. From our results, the significant anti-fungal activity of *O. gratissimum* and *O. sanctum* EOs suggest their potential applications as eco-friendly and natural antifungal agents, and therefore should be considered while devising strategies for the management of crop protection. Moreover, the plants containing EOs have been used traditionally as a green manure because of their positive outcomes as bio-stimulants, antimicrobial agent, antifeedant activities, as well as fertilizers [41,42]. In addition, several studies also have documented the beneficial effects of EO's volatile compounds on plants growing in stressful conditions [43–45]. For instance, monoterpene and isothiocyanate are known to trigger the expression of heat shock protein to alleviate heat stress in plants. As the role of HSP is not only confined to heat stress, but rather is also involved in multiple abiotic stress responses and seed vigour [46–48], it thus accentuates the significance of EO's volatile compounds for crop stress management.

As the EOs exhibited promising antimicrobial activity, we were intrigued to evaluate their antioxidant potential. To assess the antioxidant property of the EOs, we determined the ability of the EOs to scavenge the DPPH free radical. Interestingly, we observed that the EO with the highest antimicrobial activity also displayed higher DPPH free radical scavenging potential. The EO1 and EO3 effective concentration to scavenge 50% of DPPH free radical (EC50) was 9.43 ng/mL and 9.48 ng/mL, respectively, while the EC50 of EO2 was much higher, around 92.6 ng/mL (Figure 5). Furthermore, the correlation coefficient for the antioxidant activity and the antimicrobial activity was found in the range of 0.77 to 0.99. Thus, this observation suggests a significant correlation between the antimicrobial and antioxidant activity of three EOs. An antioxidant activity in the EO isolated from *O. basilicum* has been reported previously, where it was found to protect the cadmium induced DNA damage through scavenging of nitric oxide and superoxide anion free radicals [49]. Similarly, Güez et al. [50] also reported that *Ocimum* extract is a potential source of antioxidant and showed that the extract can successfully offset the effects of H_2O_2.

Table 2. The minimum inhibitory concentration of EOs as an antibacterial agent.

	Minimum Inhibitory Concentration (*v*/*v*)		
	Staphylococcus aureus	***Escherichia coli***	***Enterobacter cloacae***
EO1	12.5	6.25	25
EO2	25	25	25
EO3	12.5	12.5	25

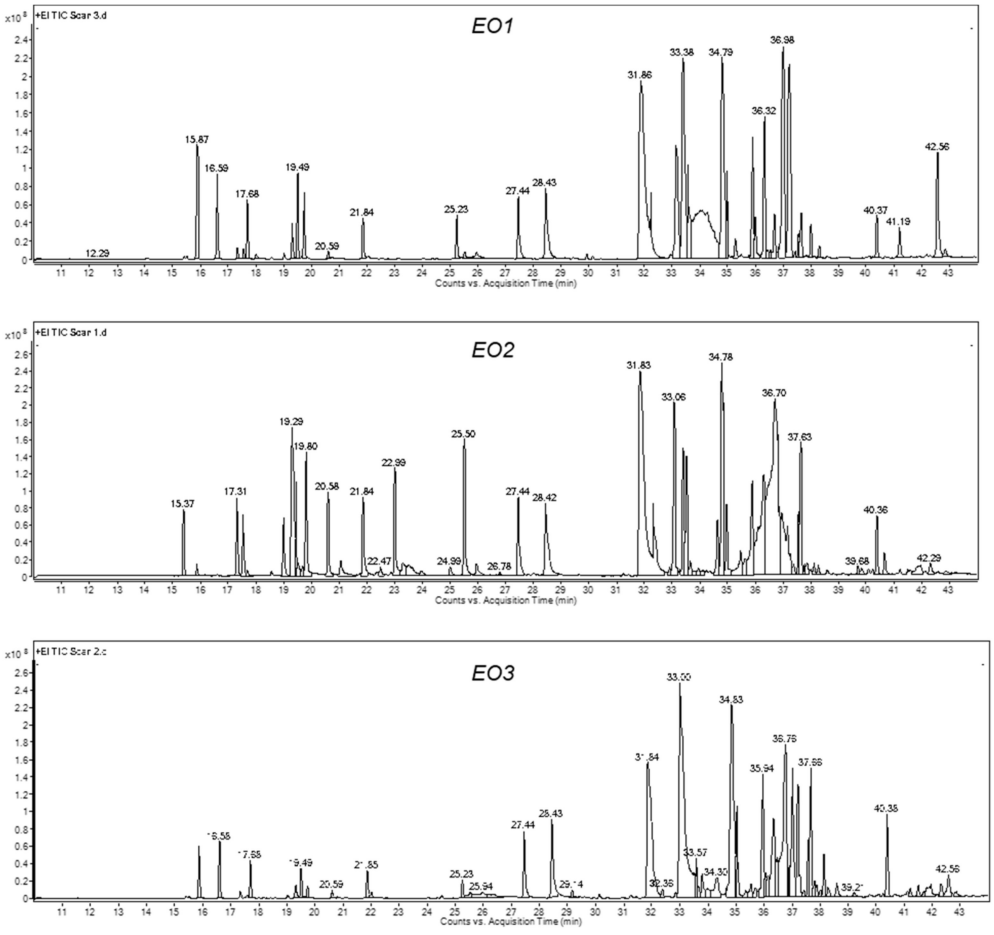

Figure 2. GC-MS chromatogram showing the separation pattern of essential oil from *O. gratissimum* (EO1), *O. tenuiflorum* (EO2), and *O. sanctum* (EO3).

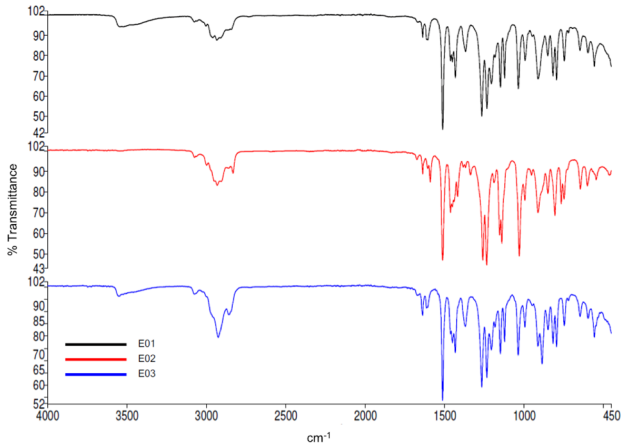

Figure 3. FT-IR spectrum of the essential oil from *O. gratissimum* (EO1, Black), *O. tenuiflorum* (EO2, Red), and *O. sanctum* (EO3, Blue).

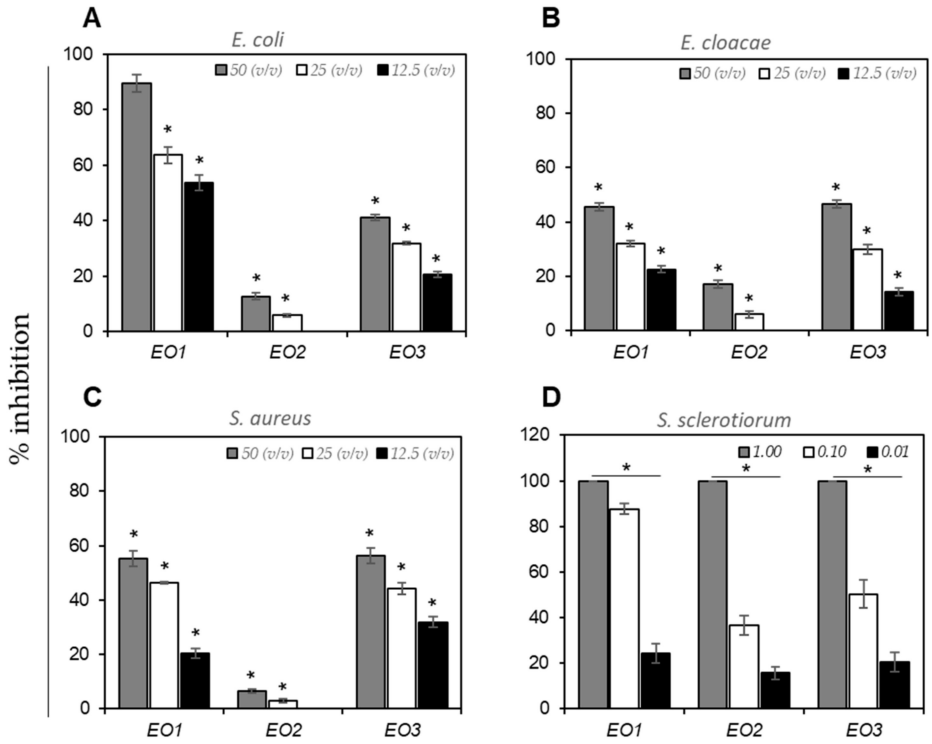

Figure 4. Antimicrobial activity of essential oil from *O. gratissimum* (EO1), *O. tenuiflorum* (EO2), and *O. sanctum* (EO3) against two-gram negative (**A**) *Escherichia coli* (ATCC 11775) and (**B**) *Enterobacter cloacae*, (ATCC 13047), gram-positive bacteria viz. methicillin resistant (**C**) *Staphylococcus aureus* (ATCC 33591), and plant fungal pathogen (**D**) *S. sclerotiorum*. The antibacterial activity of EOs is relative to antibacterial activity of Chloramphenicol (10 mcg). The analysis was performed in triplicate, and the error bar represent the standard deviation. The *p*-value indicate the statistical significance as determined through Student's *t*-test (* $p < 0.05$).

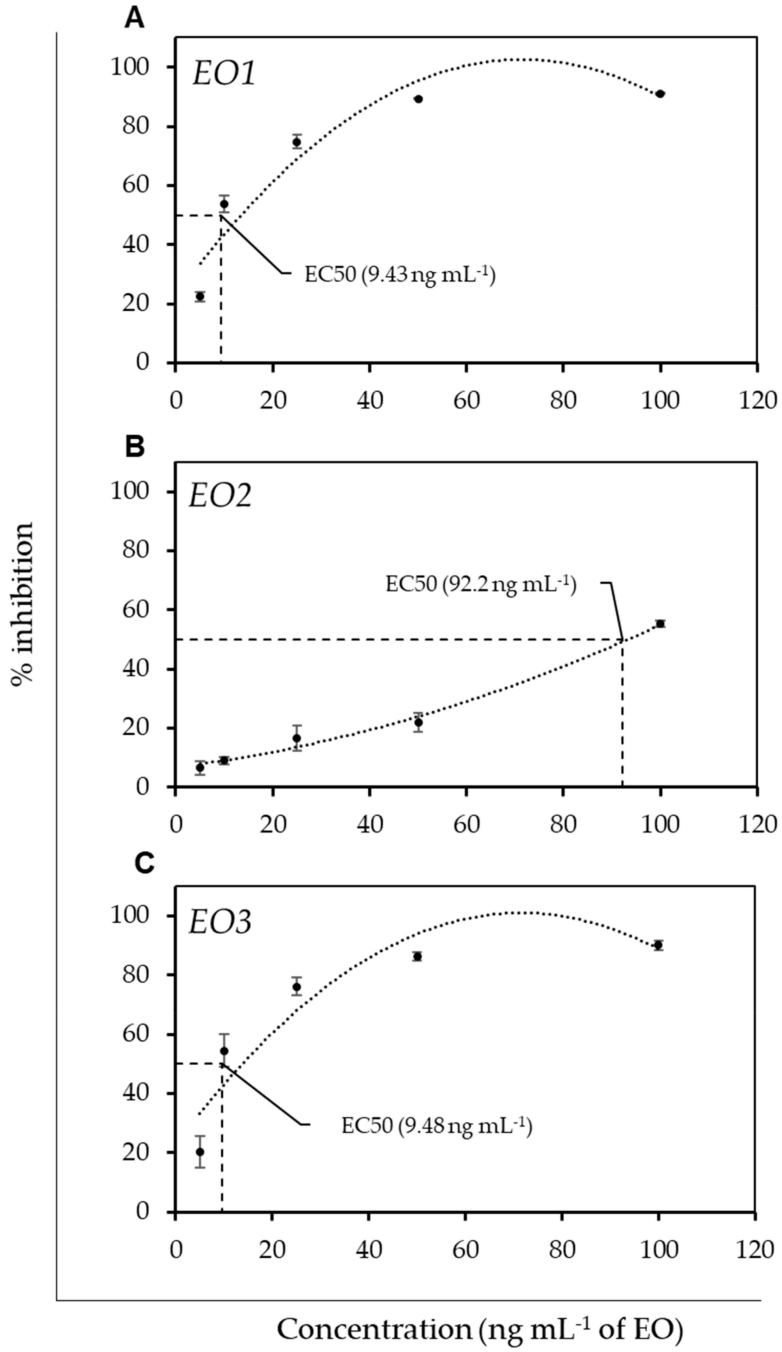

Figure 5. Comparison of antioxidant activity of essential oil from *O. gratissimum* (EO1, (**A**)), *O. tenuiflorum* (EO2, (**B**)), and *O. sanctum* (EO3, (**C**)) via DPPH radical scavenging activity.

From the biochemical characterization of EOs, it can be speculated that the compositional similarity in EO1 and EO3 may be attributed to their relatively higher antioxidant and antimicrobial activity to that of EO2. For instance, the GC-MS analysis revealed the enrichment of Phenol, 2-methoxy-3-(2-propenyl)- in EO1 (14.71%) and EO3 (8.52%), and the abundance of this bioactive compound is responsible for higher antioxidant activity [51]. Similarly, the abundance of γ-Muurolene in EO1 (6.57%) and EO3 (7.43%) may be responsible for higher antibacterial activity against *E. coli* [52]. Likewise, the presence of β-Pinene (4.86%) and -Pinene (3.11%), and β-Caryophyllene oxide (2.67%) and β-Caryophyllene (8.91%) in EO1 and EO3, respectively, may be attributed to the higher antimicrobial and antioxidant activity of these oils [53–55]. Thus, the presence of these candidate anti-fungal

or anti-bacterial compound in the EO of *Ocimum* makes it a potential source of bioactive components that can be exploited as antimicrobial agent.

3.3. In-Silico Evaluation of Antimicrobial Potential of EO

To understand the molecular basis of antimicrobial activity imparted by EOs of the *Ocimum* sp., we further conducted the in-silico assessment of the phytoconstituents using a molecular docking approach. As antibiotics target the microbial metabolism by deactivating the vital enzymes involved in biosynthesis and repair of cell walls, proteins, and nucleic-acids they restrict microbial growth. Therefore, we employed the in-silico approach to investigate the interaction of EO constituents against some vital enzymes of bacteria such as DNA gyrase, topoisomerase 4, penicillin-binding protein, dihydrofolate reductase (DHFR) and dihydropteroate synthase. These enzymes were selected due to their crucial roles in microbial metabolism and that they are potential targets of known anti-microbial agents. We performed in-silico interaction analysis of these proteins with that of 13 phytoconstituents present in the EOs of three species of *Ocimum*. The selection of the phytoconstituents for molecular docking analysis was based on their presence either in all three Eos, or their uniqueness to any of the EOs, and a few compounds were also considered based on their higher or lower concentration. Thus, the 13 selected compounds allowed us to represent differential phytoconstituents of all three EOs. The interactions were then also compared to well-known antibiotics viz. ciprofloxacin, cephalosporin, trimethoprim, and sulfonamides that are known for targeting DNA-gyrase/topoisomerase 4, penicillin-binding protein, DHFR and dihydropteroate synthetase, respectively.

The DNA gyrase consists of two protein subunits; subunit A and subunit B, that nicks the DNA and triggers negative supercoiling, respectively, and eventually resealing of DNA by the former subunit [56]. The antibiotic ciprofloxacin binds to the subunit A and restricts its activity [57]. In gram-positive bacteria, topoisomerase 4 catalyse the separation of daughter strands following replication [58]. Ciprofloxacin also shows high affinity towards the topoisomerase-4 and restricts its activity. The damaged DNA is further cleaved by endonuclease, and thus eventually leads to the bactericidal action of ciprofloxacin. The molecular docking analysis revealed that the two phytoconstituents viz. β-cubebene (-6.7 kcal mol^{-1}) and Ylangene (-6.7 kcal mol^{-1}) showed strong binding affinity towards DNA-gyrase, while three phytoconstituents viz. β-cubebene (-6.7 kcal mol^{-1}), caryophyllene oxide (-6.7 kcal mol^{-1}) and Ylangene (-6.7 kcal mol^{-1}) showed strong binding affinity towards topoisomerase 4 that is comparable to the binding affinity of ciprofloxacin (-7.1 kcal mol^{-1} for DNA-gyrase and -7.4 kcal mol^{-1} for topoisomerase 4) (Table 3).

Penicillin-binding proteins (PBPs) catalyse the formation of cross-linked peptidoglycan, an important component of bacterial cell wall. All PBPs have a N-terminal trans-glycosylase domain and a penicillin-sensitive C-terminal transpeptidase domain [59]. The antibiotic cephalosporins contains a β-lactam ring that inactivates the PBPs. The inactivation of PBPs restricts the cell wall formation that eventually stop the bacterial growth. Our in-silico analysis revealed that the three phytoconstituents viz. β-cubebene (-6.5 kcal mol^{-1}), caryophyllene oxide (-6.5 kcal mol^{-1}) and Ylangene (-6.5 kcal mol^{-1}) have comparatively strong binding affinity towards PBPs to that of cephalosporins (-6.1 kcal mol^{-1}) (Table 3). Dihydrofolate reductase is an enzyme of thymidine synthesis pathway. Trimethoprim is an antibiotic that binds to the DHFR and inhibits the synthesis of thymidine that eventually affects the DNA-synthesis [60]. The *Ocimum* EO has two compounds that exhibit higher in-silico binding affinity towards DHFR than the trimethoprim itself; -β-cubebene and β-caryophyllene oxide had binding energy of -7.6 kcal mol^{-1} and -7.8 kcal mol^{-1}, respectively, while trimethoprim has only -7.5 kcal mol^{-1} (Table 3). The sulfamethoxazole antibiotic competes with para-amino benzoic acid PABA for binding with the dihydropteroate synthetase with much greater affinity and inhibits the formation of dihydrofolic acid. The inhibition of dihydrofolic acid formation affects the DNA synthesis. β-cubebene has shown the similar affinity towards dihydropteroate synthetase with binding energy of -6.1 kcal mol^{-1} in comparison to the binding affinity of sulfamethoxazole which has shown its affinity with -6.2 kcal mol^{-1}.

Table 3. Molecular docking/in-silico analysis illustrating the comparative binding energy (kcal mol^{-1}) for interaction of key metabolic enzymes of bacterial with phytoconstituents present in the EOs of three species of *Ocimum* and known antibiotics viz. ciprofloxacin, cephalosporin, trimethoprim and sulfonamides.

Compounds	DNA-Gyrase	Topoisomerase-4	Dihydrofolate Reductase	Penicillin Binding Protein	Dihydropteroate Synthase
	Binding Energy (kcal mol^{-1})				
Eucalyptol	−4.6	−5.3	−5.9	−5.8	−4.8
Eugenol	−5.1	−5.4	−6.0	−4.6	−4.8
Linalool	−4.9	−4.7	−5.4	−4.3	−4.4
γ-terpinene	−5.8	−5.3	−5.6	−5.6	−4.7
β-Phellandrene	−5.7	−5.2	−5.7	−5.7	−5.2
β-Pinene	−4.7	−5.1	−5.7	−5.7	−5.3
β-ocimene	−5.3	−4.7	−5.4	−4.7	−4.3
Borneol	−4.6	−5.4	−5.4	−4.6	−5.0
1R-α-pinene	−4.6	−5.9	−5.7	−5.0	−4.5
β-cubebene	−6.7	−6.7	−7.6	−6.5	−6.1
α-citral	−4.7	−4.0	−5.1	−4.7	−4.4
caryophyllene oxide	−5.6	−6.7	−7.8	−6.5	−5.8
Ylangene	−6.7	−6.7	−7.2	−6.5	−6.0
Ciprofloxacin	−7.1	−7.4	-	-	-
Trimethoprim	-	-	−7.5	-	-
Sulfamethoxazole	-	-	-	-	−6.2
Cephalosporin	-	-	-	−6.1	-

To see the 2D and 3D visuals of interactions between the target proteins and the phytoconstituents we used PyMol and discovery studio visualizer. As the binding energy of caryophyllene oxide with DHFR was higher (−7.8 kcal/mol) than that of trimethoprim (−7.5 kcal/mol), we analysed the 2D and 3D model of docked trimethoprim or caryophyllene oxide to DHFR that depicts the effective binding of caryophyllene oxide than trimethoprim (Figure 6A). Briefly, the interaction of trimethoprim with DHFR involves amino acid residues Leu 21, Phe 93, Phe 99, Thr 47, Val 7, while in the same active site caryophyllene oxide interact with Leu 21, Val 7, Ala 8, etc. (Figure 6B).

Thus, based on molecular docking we can speculate that phytoconstituents with the lower binding energy as compared to known antibiotic compounds would be more effective in terms of antimicrobial inhibition. Besides, if not effective these phytoconstituents can also be utilized as new antimicrobial agents. In a recent study, Aliye et al. (2021) [61] did a molecular docking analysis on phytoconstituents from essential oil extracted from the leaves and roots of *Ocimum cufodontii*, which is an important plant in Ethiopia due to its pharmacological role. The phytoconstituents revealed from GC-MS were examined in-silico (molecular docking) with DNA-Gyrase, an important bacterial enzyme. The in-silico analysis clearly revealed the interaction between compounds from the oil extract and the DNA-Gyrase with better binding affinity suggesting that these beneficial compounds may serve as possible anti-microbial agents. Similarly, Silva et al. (2020) [62] found that the potential compounds from essential oils of different plants show binding affinity towards several important proteins of SARS-COV2 and proposed that these compounds may serve as potential anti-viral agents. The upsurge in the rate of antimicrobial resistance demands the identification and characterization of biomolecules that can be employed for strategic drug design. Antibiotics have been developed to control and prevent infections caused by microbes however, microbial infections are still a major challenge across the globe. Therefore, these biomolecules with higher binding affinity might play an instrumental role in antibacterial activity.

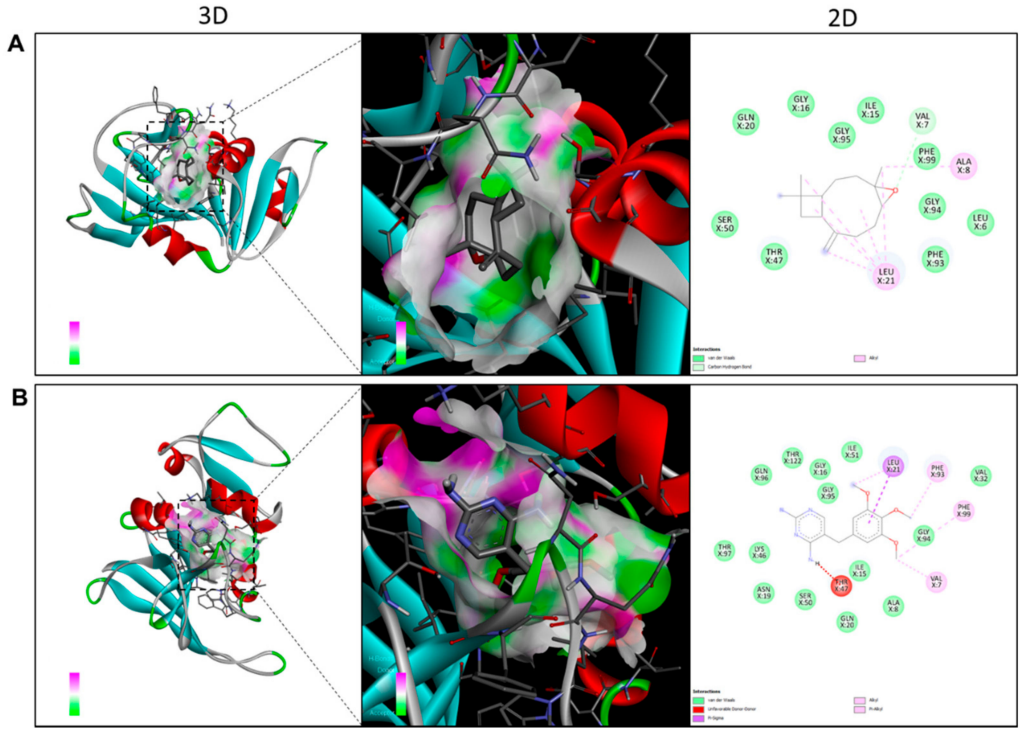

Figure 6. 2D and 3D diagrams illustrating the binding patterns of the (**A**) caryophyllene oxide, and (**B**) trimethoprim into the active site of Dihydrofolate Reductase (PDB ID- 3SRW) showing H-bond donor (pink) and acceptor (green) surfaces in the docked complex.

4. Conclusions

The volatile nature of EOs is attributed to diverse secondary metabolites produced by aromatic plants. These volatile compounds are known for their antioxidant and antimicrobial potential. In the present study, we have explored the antimicrobial potential of the EOs isolated from species of *Ocimum*, which are a known resource for natural bioactive metabolites. The EOs showed significant microbial inhibition, and their antimicrobial activity was well correlated with their antioxidant potential. The biochemical assessment the EOs also revealed that the EOs were enriched in diverse bioactive compounds such as Phenol, 2-methoxy-3-(2-propenyl), γ-Muurolene, Ylangene, β-Cubebene, etc. Besides, an in-silico analysis of the candidate bioactive compounds using molecular docking further supported the antimicrobial role of the EOs. As suggested by several studies, the individual isolated compounds were not as effective as the entire extract/or the EO due to the synergistic implication of different bioactive compounds. Therefore, it is important to explore the major phytoconstituents whose combination might have role as antimicrobial agent.

Hence, the purification, and characterization of the major bioactive components of the crude extract is required to decrypt the key candidate compounds associated with the antimicrobial function.

Author Contributions: Conceptualization, P.S. and G.K.; data curation, N.G., A.V., N.R., K. and V.G.; formal analysis, P.S., G.K. and S.R.; writing—original draft, G.K. and P.S.; writing—review and editing, G.K. and P.S. All authors have read and agreed to the published version of the manuscript.

Funding: P.S. and G.K. acknowledge research funding from the Department of Science and Technology in the form of the INSPIRE faculty awards (DST/INSPIRE/04/2018/003425 and DST/INSPIRE/04/2016/002489, respectively). G.K. also acknowledges SERB, DST, Govt. of India for providing financial support under the scheme of Early Career Research Award (ECR/2018/002364).

Data Availability Statement: The data presented in this study are available in the present article.

Acknowledgments: We gratefully acknowledge the Executive Director, NABI, Mohali for constant support. The authors also thank the Centre for Aromatic Plants, Dehradun, India for providing essential oil used in this study.

Conflicts of Interest: The authors declare no conflict of interest.

References

1. Tripathi, P.; Singh, A. *Chapter 19—Biofertilizers: "An Ace in the Hole" in Medicinal and Aromatic Plants Cultivation*; Rakshit, A., Meena, V.S., Parihar, M., Singh, H.B., Singh, A.K.B.T.-B., Eds.; Woodhead Publishing: Sawston, UK, 2021; Volume 1, pp. 253–263. ISBN 978-0-12-821667-5.
2. Aftab, T. A review of medicinal and aromatic plants and their secondary metabolites status under abiotic stress. *J. Med. Plants* **2019**, *7*, 99–106.
3. Wallace, R.J. Antimicrobial properties of plant secondary metabolites. *Proc. Nutr. Soc.* **2004**, *63*, 621–629. [CrossRef] [PubMed]
4. Figueiredo, A.C.; Barroso, J.G.; Pedro, L.G.; Scheffer, J.J.C. Factors affecting secondary metabolite production in plants: Volatile components and essential oils. *Flavour Fragr. J.* **2008**, *23*, 213–226. [CrossRef]
5. Rehman, R.; Hanif, M.A.; Mushtaq, Z.; Al-Sadi, A.M. Biosynthesis of essential oils in aromatic plants: A review. *Food Rev. Int.* **2016**, *32*, 117–160. [CrossRef]
6. Gounaris, Y. Biotechnology for the production of essential oils, flavours and volatile isolates. A review. *Flavour Fragr. J.* **2010**, *25*, 367–386. [CrossRef]
7. Batish, D.R.; Singh, H.P.; Kohli, R.K.; Kaur, S. Eucalyptus essential oil as a natural pesticide. *For. Ecol. Manag.* **2008**, *256*, 2166–2174. [CrossRef]
8. Nazzaro, F.; Fratianni, F.; De Martino, L.; Coppola, R.; De Feo, V. Effect of essential oils on pathogenic bacteria. *Pharmaceuticals* **2013**, *6*, 1451–1474. [CrossRef]
9. Matasyoh, J.C.; Kiplimo, J.J.; Karubiu, N.M.; Hailstorks, T.P. Chemical composition and antimicrobial activity of essential oil of Tarchonanthus camphoratus. *Food Chem.* **2007**, *101*, 1183–1187. [CrossRef]
10. Hazzoumi, Z.; Moustakime, Y.; Joutei, K.A. Effect of arbuscular mycorrhizal fungi (AMF) and water stress on growth, phenolic compounds, glandular hairs, and yield of essential oil in basil (*Ocimum gratissimum* L). *Chem. Biol. Technol. Agric.* **2015**, *2*, 10. [CrossRef]
11. Kumar, B.; Bajpai, V.; Tiwari, S.; Pandey, R. *Phytochemistry of Plants of Genus Ocimum*, 1st ed.; CRC Press: Boca Raton, FL, USA; New York, NY, USA, 2020; pp. 1–77. ISBN 1003014852.
12. Singh, D.; Chaudhuri, P.K. A review on phytochemical and pharmacological properties of Holy basil (*Ocimum sanctum* L.). *Ind. Crops Prod.* **2018**, *118*, 367–382. [CrossRef]
13. Rastogi, S.; Shah, S.; Kumar, R.; Vashisth, D.; Akhtar, M.Q.; Kumar, A.; Dwivedi, U.N.; Shasany, A.K. Ocimum metabolomics in response to abiotic stresses: Cold, flood, drought and salinity. *PLoS ONE* **2019**, *14*, e0210903. [CrossRef]
14. Rastogi, S.; Shah, S.; Kumar, R.; Kumar, A.; Shasany, A.K. Comparative temporal metabolomics studies to investigate interspecies variation in three Ocimum species. *Sci. Rep.* **2020**, *10*, 5234. [CrossRef]
15. Reddy, D.N. Essential oils extracted from medicinal plants and their applications. In *Natural Bio-Active Compounds*, 1st ed.; Akhtar, M., Swamy, M., Sinniah, U., Eds.; Springer: Singapore, 2019; Volume 1, pp. 237–283.
16. Dhama, K.; Sharun, K.; Gugjoo, M.B.; Tiwari, R.; Alagawany, M.; Iqbal Yatoo, M.; Thakur, P.; Iqbal, H.M.N.; Chaicumpa, W.; Michalak, I. A comprehensive review on chemical profile and pharmacological activities of Ocimum basilicum. *Food Rev. Int.* **2021**, 1–29. [CrossRef]
17. Kaur, H.; Manna, M.; Thakur, T.; Gautam, V.; Salvi, P. Imperative role of sugar signaling and transport during drought stress responses in plants. *Physiol. Plant.* **2021**, *171*, 833–848. [CrossRef]
18. Salvi, P.; Manna, M.; Kaur, H.; Thakur, T.; Gandass, N.; Bhatt, D.; Muthamilarasan, M. Phytohormone signaling and crosstalk in regulating drought stress response in plants. *Plant Cell Rep.* **2021**, *40*, 1305–1329. [CrossRef]
19. Manna, M.; Thakur, T.; Chirom, O.; Mandlik, R.; Deshmukh, R.; Salvi, P. Transcription factors as key molecular target to strengthen the drought stress tolerance in plants. *Physiol. Plant.* **2021**, *172*, 847–868. [CrossRef]
20. Dresselhaus, T.; Hückelhoven, R. Biotic and abiotic stress responses in crop plants. *Agronomy* **2018**, *8*, 267. [CrossRef]
21. Salvi, P.; Agarrwal, R.; Kajal; Gandass, N.; Manna, M.; Kaur, H.; Deshmukh, R. Sugar transporters and their molecular tradeoffs during abiotic stress responses in plants. *Physiol. Plant.* **2022**, e13652. [CrossRef]
22. Hasanuzzaman, M.; Mohsin, S.M.; Bhuyan, M.H.M.B.; Bhuiyan, T.F.; Anee, T.I.; Masud, A.A.C.; Nahar, K. Phytotoxicity, environmental and health hazards of herbicides: Challenges and ways forward. In *Agrochemicals Detection, Treatment and Remediation*; Elsevier: Amsterdam, The Netherlands, 2020; pp. 55–99.
23. AL-Ahmadi, M.S. Pesticides, anthropogenic activities, and the health of our environment safety. In *Pesticides-Use and Misuse and Their Impact in the Environment*; Larramendy, M., Soloneski, S., Eds.; IntechOpen: London, UK, 2019; pp. 1–23.
24. Duran-Lara, E.F.; Valderrama, A.; Marican, A. Natural organic compounds for application in organic farming. *Agriculture* **2020**, *10*, 41. [CrossRef]
25. Rothmann, L.A.; McLaren, N.W. Sclerotinia sclerotiorum disease prediction: A review and potential applications in South Africa. *S. Afr. J. Sci.* **2018**, *114*, 1–9. [CrossRef]

26. O'Sullivan, C.A.; Belt, K.; Thatcher, L.F. Tackling control of a cosmopolitan phytopathogen: Sclerotinia. *Front. Plant Sci.* **2021**, *12*, 1764. [CrossRef] [PubMed]
27. Peltier, A.J.; Bradley, C.A.; Chilvers, M.I.; Malvick, D.K.; Mueller, D.S.; Wise, K.A.; Esker, P.D. Biology, yield loss and control of Sclerotinia stem rot of soybean. *J. Integr. Pest Manag.* **2012**, *3*, B1–B7. [CrossRef]
28. Adams, R.P. *Identification of Essential oil Components by Gas Chromatography/Mass Spectrometry*, 4th ed.; Allured Publishing Corporation Carol Stream: Carol Stream, IL, USA, 2007; Volume 456.
29. Joshi, R.K. Chemical composition, in vitro antimicrobial and antioxidant activities of the essential oils of Ocimum gratissimum, O. sanctum and their major constituents. *Indian J. Pharm. Sci.* **2013**, *75*, 457. [CrossRef] [PubMed]
30. Siddharth, S.; Vittal, R.R. Evaluation of antimicrobial, enzyme inhibitory, antioxidant and cytotoxic activities of partially purified volatile metabolites of marine Streptomyces sp. S2A. *Microorganisms* **2018**, *6*, 72. [CrossRef]
31. Trott, O.; Olson, A.J. AutoDock Vina: Improving the speed and accuracy of docking with a new scoring function, efficient optimization, and multithreading. *J. Comput. Chem.* **2010**, *31*, 455–461. [CrossRef]
32. Guex, N.; Peitsch, M.C. SWISS-MODEL and the Swiss-Pdb Viewer: An environment for comparative protein modeling. *Electrophoresis* **1997**, *18*, 2714–2723. [CrossRef]
33. Morris, G.M.; Huey, R.; Lindstrom, W.; Sanner, M.F.; Belew, R.K.; Goodsell, D.S.; Olson, A.J. AutoDock4 and AutoDockTools4: Automated docking with selective receptor flexibility. *J. Comput. Chem.* **2009**, *30*, 2785–2791. [CrossRef]
34. Stefan, M.; Zamfirache, M.M.; Padurariu, C.; Trută, E.; Gostin, I. The composition and antibacterial activity of essential oils in three Ocimum species growing in Romania. *Cent. Eur. J. Biol.* **2013**, *8*, 600–608. [CrossRef]
35. Hzounda, J.B.F.; Jazet, P.M.D.; Lazar, G.; Răducanu, D.; Caraman, I.; Bassene, E.; Boyom, F.F.; Lazar, I.M. Spectral and chemometric analyses reveal antioxidant properties of essential oils from four Cameroonian Ocimum. *Ind. Crops Prod.* **2016**, *80*, 101–108. [CrossRef]
36. Schulz, H.; Schrader, B.; Quilitzsch, R.; Pfeffer, S.; Krüger, H. Rapid classification of basil chemotypes by various vibrational spectroscopy methods. *J. Agric. Food Chem.* **2003**, *51*, 2475–2481. [CrossRef]
37. Schulz, H.; Baranska, M. Identification and quantification of valuable plant substances by IR and Raman spectroscopy. *Vib. Spectrosc.* **2007**, *43*, 13–25. [CrossRef]
38. Jadhav, S.; Shah, R.; Bhave, M.; Palombo, E.A. Inhibitory activity of yarrow essential oil on Listeria planktonic cells and biofilms. *Food Control* **2013**, *29*, 125–130. [CrossRef]
39. Khan, A.; Ahmad, A.; Akhtar, F.; Yousuf, S.; Xess, I.; Khan, L.A.; Manzoor, N. Ocimum sanctum essential oil and its active principles exert their antifungal activity by disrupting ergosterol biosynthesis and membrane integrity. *Res. Microbiol.* **2010**, *161*, 816–823. [CrossRef]
40. Žabka, M.; Pavela, R.; Kovaříková, K.; Tříska, J.; Vrchotová, N.; Bednář, J. Antifungal and Insecticidal Potential of the Essential Oil from Ocimum sanctum L. against Dangerous Fungal and Insect Species and Its Safety for Non-Target Useful Soil Species Eisenia fetida (Savigny, 1826). *Plants* **2021**, *10*, 2180. [CrossRef]
41. Raut, J.S.; Karuppayil, S.M. A status review on the medicinal properties of essential oils. *Ind. Crops Prod.* **2014**, *62*, 250–264. [CrossRef]
42. Raveau, R.; Fontaine, J.; Lounès-Hadj Sahraoui, A. Essential oils as potential alternative biocontrol products against plant pathogens and weeds: A review. *Foods* **2020**, *9*, 365. [CrossRef]
43. Hara, M.; Yamauchi, N.; Sumita, Y. Monoterpenes induce the heat shock response in Arabidopsis. *Z. Für Naturforsch. C* **2018**, *73*, 177–184. [CrossRef]
44. Hara, M.; Harazaki, A.; Tabata, K. Administration of isothiocyanates enhances heat tolerance in Arabidopsis thaliana. *Plant Growth Regul.* **2013**, *69*, 71–77. [CrossRef]
45. Yamauchi, Y.; Kunishima, M.; Mizutani, M.; Sugimoto, Y. Reactive short-chain leaf volatiles act as powerful inducers of abiotic stress-related gene expression. *Sci. Rep.* **2015**, *5*, 8030. [CrossRef]
46. Wang, W.; Vinocur, B.; Shoseyov, O.; Altman, A. Role of plant heat-shock proteins and molecular chaperones in the abiotic stress response. *Trends Plant Sci.* **2004**, *9*, 244–252. [CrossRef]
47. Mishra, D.; Shekhar, S.; Singh, D.; Chakraborty, S.; Chakraborty, N. Heat shock proteins and abiotic stress tolerance in plants. In *Regulation of Heat Shock Protein Responses*; Asea, A., Kaur, P., Eds.; Springer: Singapore, 2018; Volume 13, pp. 41–69.
48. Kaur, H.; Petla, B.P.; Kamble, N.U.; Singh, A.; Rao, V.; Salvi, P.; Ghosh, S.; Majee, M. Differentially expressed seed aging responsive heat shock protein OsHSP18.2 implicates in seed vigor, longevity and improves germination and seedling establishment under abiotic stress. *Front. Plant Sci.* **2015**, *6*, 713. [CrossRef] [PubMed]
49. Thirugnanasampandan, R.; Jayakumar, R. Protection of cadmium chloride induced DNA damage by Lamiaceae plants. *Asian Pac. J. Trop. Biomed.* **2011**, *1*, 391–394. [CrossRef]
50. Güez, C.M.; de Souza, R.O.; Fischer, P.; Leão, M.F.d.M.; Duarte, J.A.; Boligon, A.A.; Athayde, M.L.; Zuravski, L.; de Oliveira, L.F.S.; Machado, M.M. Evaluation of basil extract (*Ocimum basilicum* L.) on oxidative, anti-genotoxic and anti-inflammatory effects in human leukocytes cell cultures exposed to challenging agents. *Braz. J. Pharm. Sci.* **2017**, *53*, e15098. [CrossRef]
51. Kabuto, H.; Tada, M.; Kohno, M. Eugenol [2-methoxy-4-(2-propenyl) phenol] prevents 6-hydroxydopamine-induced dopamine depression and lipid peroxidation inductivity in mouse striatum. *Biol. Pharm. Bull.* **2007**, *30*, 423–427. [CrossRef]
52. Perigo, C.V.; Torres, R.B.; Bernacci, L.C.; Guimaraes, E.F.; Haber, L.L.; Facanali, R.; Vieira, M.A.R.; Quecini, V.; Marques, M.O.M. The chemical composition and antibacterial activity of eleven Piper species from distinct rainforest areas in Southeastern Brazil. *Ind. Crops Prod.* **2016**, *94*, 528–539. [CrossRef]

53. Salehi, B.; Upadhyay, S.; Erdogan Orhan, I.; Kumar Jugran, A.; Jayaweera, S.L.D.; Dias, D.A.; Sharopov, F.; Taheri, Y.; Martins, N.; Baghalpour, N. Therapeutic potential of α-and β-pinene: A miracle gift of nature. *Biomolecules* **2019**, *9*, 738. [CrossRef]
54. Singh, G.; Marimuthu, P.; De Heluani, C.S.; Catalan, C.A.N. Antioxidant and biocidal activities of Carum nigrum (seed) essential oil, oleoresin, and their selected components. *J. Agric. Food Chem.* **2006**, *54*, 174–181. [CrossRef]
55. Sabulal, B.; Dan, M.; Kurup, R.; Pradeep, N.S.; Valsamma, R.K.; George, V. Caryophyllene-rich rhizome oil of Zingiber nimmonii from South India: Chemical characterization and antimicrobial activity. *Phytochemistry* **2006**, *67*, 2469–2473. [CrossRef]
56. Reece, R.J.; Maxwell, A. DNA gyrase: Structure and function. *Crit. Rev. Biochem. Mol. Biol.* **1991**, *26*, 335–375. [CrossRef]
57. Collin, F.; Karkare, S.; Maxwell, A. Exploiting bacterial DNA gyrase as a drug target: Current state and perspectives. *Appl. Microbiol. Biotechnol.* **2011**, *92*, 479–497. [CrossRef]
58. Drlica, K.; Zhao, X. DNA gyrase, topoisomerase IV, and the 4-quinolones. *Microbiol. Mol. Biol. Rev.* **1997**, *61*, 377–392.
59. Basu, J.; Chattopadhyay, R.; Kundu, M.; Chakrabarti, P. Purification and partial characterization of a penicillin-binding protein from Mycobacterium smegmatis. *J. Bacteriol.* **1992**, *174*, 4829–4832. [CrossRef]
60. Schweitzer, B.I.; Dicker, A.P.; Bertino, J.R. Dihydrofolate reductase as a therapeutic target. *FASEB J.* **1990**, *4*, 2441–2452. [CrossRef]
61. Aliye, M.; Dekebo, A.; Tesso, H.; Abdo, T.; Eswaramoorthy, R.; Melaku, Y. Molecular docking analysis and evaluation of the antibacterial and antioxidant activities of the constituents of Ocimum cufodontii. *Sci. Rep.* **2021**, *11*, 10101. [CrossRef]
62. da Silva, J.K.R.; Figueiredo, P.L.B.; Byler, K.G.; Setzer, W.N. Essential oils as antiviral agents, potential of essential oils to treat SARS-CoV-2 infection: An in-silico investigation. *Int. J. Mol. Sci.* **2020**, *21*, 3426. [CrossRef]